Carbon 130 (2018) 215–221

Contents lists available at ScienceDirect

Carbon

journal homepage: www.elsevier.com/locate/carbon

Friction-induced rapid restructuring of graphene nanocrystallite cap layer at sliding surfaces: Short run-in period

Cheng Chen, Peidong Xue, Xue Fan, Chao Wang, Dongfeng Diao*

Institute of Nanosurface Science and Engineering (INSE), Guangdong Provincial Key Laboratory of Micro/Nano Optomechatronics Engineering, Shenzhen University, Shenzhen, 518060, China

ARTICLE INFO

Article history:

ABSTRACT

Amorphous carbon film is vastly applied for low-friction protective coatings at contact sliding surfaces. However before reaching steady low friction status, the film always endures a high friction period known as the "run-in" period, sometimes taking thousands of sliding cycles, causing remarkable energy dissipation. Here, we report that the run-in period of amorphous carbon film could be drastically shortened to 22 ± 5 cycles by fabricating a 5-nm graphene nanocrystallite cap layer. The cap layer gave rise to rapid formation of graphene nanocrystallized transfer film, which responds to the short run-in period. We found two key factors for the rapid formation of transfer film. Firstly, the cap layer had lower wear resistance than the amorphous carbon, severing as a quick-wearing sacrificial layer. Secondly, the nanocrystallization of transfer film was mainly due to friction-induced restructuring of graphene nanocrystallite but not friction-induced heat. In addition, the friction test of amorphous carbon film covered with multilayer graphene micro-flakes also verified that friction-induced rapid restructuring of graphene sheets at sliding surfaces resulted in short run-in period.

1. Introduction

Amorphous carbon (a-C) film is an important class of tribological materials for its excellent properties such as low friction coefficient, high wear resistance and hardness [1–3]. It has been used worldwide as surface protective coatings in everyday devices ranging from magnetic disks to razor blades as well as manufacturing and automobile industries [3]. The low friction of a-C film can ensure long operation life of devices with minimal interruptions and negligible energy dissipation by friction. However, before reaching low friction steady stage, a-C film always has a high friction period ($\mu > 0.1$), so-called "run-in" period. The duration of run-in period is uncertain to some extent and sometimes it would take thousands of sliding cycles [4–6]. So in order to make the low-friction application more effective, the run-in period is necessary to be shortened or even eliminated.

The run-in period is a transient stage during which some sort of interfacial conditioning necessary for low friction occurs. At the beginning of friction, high friction force arises from the initial interaction between a-C surface and the counter surface. As sliding continues, the contact surface of a-C detaches, reacts, and transfers to the counterface [6]. Meanwhile, the a-C structure is transformed to the graphite-like nanocrystallite structure by the heat generated by friction and/or the stress provided by the mechanical/friction force [7–12]. Then, a graphite-like nanocrystallite transfer film forms on the counter surface, which always coincides with the decreasing of friction coefficient [13]. The formation of graphite-like nanocrystallite transfer film lowers the interaction force between the sliding surfaces from strong covalent bonds to mainly weak van der Waal forces. Hence, in order to shorten the run-in period, one feasible way is to accelerate the formation of graphite-like nanocrystallite transfer film. Many studies have shown that the formation of the transfer film was affected by sliding conditions [14–17]. At elevated temperatures, transfer films tended to form faster and shorten the run-in period [14]. High load or high sliding speed led to faster formation of transfer film and had a crucial effect on the nanostructure transformation [15,16]. Counterface material also play an important role on the formation of transfer film. Transfer film build-up faster on clean surfaces of steel pins than those that are covered by an oxide layer, as carbon film surface reacts preferentially with metallic iron [17]. However, the above sliding conditions are often uncontrollable in the low-friction application. Some researchers also pointed out that the

* Corresponding author.
E-mail address: dfdiao@szu.edu.cn (D. Diao).

https://doi.org/10.1016/j.carbon.2018.01.022
0008-6223/

surface contaminant layer [18,19], surface roughness [20] and sp^2/sp^3 ratio [21] of carbon film had effects on the length of run-in period. But few methods have been proposed for effective shortening or eliminating the run-in period.

As mentioned above, the formation of transfer film depends on the migration of carbon from a-C film to counter surface, and the nanostructural transformation from amorphous to graphite. Therefore, the main obstacles for the rapid formation of transfer film are the high wear resistance of a-C film and the pure amorphous structure without any graphene sheets for directly serving as raw material. In this study, we propose a method for facilitating the formation of transfer film and shortening the run-in period by depositing a thin graphene nanocrystallite (G-N) cap layer on the a-C film. The effects of cap layer thickness and G-N size on the run-in period were studied. Investigations of the formation of transfer films and nanoscratch tests of the carbon films were carried out to reveal the role of G-N cap layer on rapid formation of nanocrystallized transfer film. The nanostructure transformation mechanism of transfer film was discussed by comparing the annealing effects on the nanostructures of 5 nm-thick a-C film and 5 nm-thick G-N film. Multilayer graphene micro-flakes were employed to further verify the short run-in period mechanism.

2. Experimental

The a-C film and G-N cap layer were fabricated by using an electron cyclotron resonance (ECR) plasma sputtering system. The detailed description of the sputtering system was reported in our previous works [22,23]. The a-C film was deposited on silicon substrate (p-type <100>) with ion irradiation in divergent electron cyclotron resonance (DECR) plasma sputtering type [22]. The background pressure of the vacuum chamber was pumped down to 8×10^{-5} Pa and argon was inflated keeping the working pressure at 1×10^{-1} Pa. During the film deposition, ion irradiation was realized with a substrate bias voltage of −10 V. The deposition time was 30 min and the film thickness was 90 nm. The G-N cap layer was deposited on the a-C film with electron irradiation in mirror-confinement electron cyclotron resonance (MCECR) plasma sputtering type [23]. The argon working pressure was 4×10^{-2} Pa. Electron irradiation energies varied from 10 eV to 50 eV with different positive substrate biases to change the size of graphene nanocrystallite in the cap layer. The deposition time was used to control the cap layer thickness. The deposition rate was about 1 nm/min, and cap layers with thicknesses of 1 nm, 2 nm, 5 nm and 10 nm were obtained.

Multilayer (1–5 layers) graphene micro-flakes were purchased from Tanfeng Tech. Inc. Firstly, the graphene micro-flakes were suspended in ethanol. The weight concentration of graphene flakes was 10 mg/L. Then, 1 mL graphene-flake-containing ethanol solution was spread on the a-C film surface, and evaporated in the atmosphere.

The nanostructures of the carbon films were analyzed with Raman spectroscopy (HORIBA, HR-Resolution; wavelength of 532 nm) and transmission electron microscopy (TEM, JEOL, JEM-3200FS). The cross-sectional TEM specimens were cut from the films and progressively thinned to about 100 nm thick by using a focused ion beam (FIB, FEI, Scios). A Pt protective layer was deposited on the top of the specimen and the final polishing was done with a beam current of only 27 pA to avoid possible damages (including ion doping) or thermal recrystallization caused by ion bombardments.

Frictional tests of the films sliding against a Si_3N_4 ball (radius of 3.17 mm) were performed with a Pin-on-Disk tribometer. The normal load was 2 N. The sliding velocity was 26.4 mm/s, corresponding to a constant disk rotational speed of 180 rpm with a frictional radius of 1.4 mm. The tests were operated in a clean room with a temperature of 24 °C and a relative humidity of 45–50%. The tests were repeated more than five times for each film. The structures of the transfer films on the Si_3N_4 ball surfaces were analyzed with optical microscope and Raman spectroscopy. The cross-sectional nanostructure of the transfer films were observed with a Cs-corrected TEM (FEI, Titan3 Themis G2). The TEM specimens were cut out from the ball surface and were thinned to about 100 nm by using the FIB. Au and Pt layers were subsequently deposited on the specimens to make them conductive and protect from possible damage.

The nanoscratch tests of the carbon films were carried out with an atomic force microscope (AFM, Bruker, Dimension edge). A stainless steel cantilever with an 80 nm-radius diamond tip was attached to the cantilever holder of the AFM. The scratch normal load was 200 μN. The nanoindentation tests of the carbon films were performed with a nanoindenter (Hysitron, TI-950). A Berkovich diamond indenter with a tip radius of 100 nm was used and the maximum load for indentation was 500 μN. A pre-test on quartz standard sample was done to calibrate the equipment. The value of hardness was given by averaging five different measurement results. The annealing experiments of 5 nm-thick a-C film and 5 nm-thick G-N film were performed with a tube heating furnace under 1 L/min flowing argon gas. The films were heated from room temperature to 500 °C, 750 °C, 1000 °C in 20 min, then kept for 30 min. The films were naturally cooled to RT after annealing.

3. Results and discussion

3.1. Effect of G-N cap layer on run-in period of friction

The cross-sectional TEM images of a-C film and a-C film with G-N cap layer (electron irradiation energy, 40 eV; deposition time, 5 min) are shown in Fig. 1(a). It can be seen that the thicknesses of the a-C film and G-N cap layer were 90 nm and the 5 nm, respectively. The enlargement TEM images of region I and region II show that a-C film was pure amorphous structure and the cap layer was consisted of sheets stacks. The interplanar spacing of the sheet was approximately 0.36 nm, matches the interplanar spacing of graphene sheets. The orientation of graphene sheets was perpendicular to the substrate. Comparing Raman spectra of the two films, as shown in Fig. 1(b), a sharp D peak appeared with the existence of G-N cap layer, which further indicates that the nanostructure of the G-N cap layer was nanocrystallite. Fig. 1(c) shows the typical friction curves of the a-C film and a-C film with G-N cap layer. The friction coefficient of the a-C film was about 0.20 at the beginning, then slowly decreased to a stable lower value of 0.06 after about 470 sliding cycles. The run-in period of the a-C film is about 470 cycles. For the a-C film with G-N cap layer, friction coefficient rapidly reduced to stable value of 0.06 with only 17 cycles. These results indicate that the run-in period of amorphous carbon film could be significantly shortened with G-N cap layer.

G-N cap layers with different G-N sizes and layer thicknesses were fabricated by varying irradiation energy and deposition time to systematically investigate the effect of G-N cap layer on the reduction of run-in period. The ratio of D band to G band (I_D/I_G) was obtained by fitting the D band and G band of Raman spectrum with a Lorentzian line and a Breit-Fano-Wagner (BFW) line, respectively. According to the three-stage amorphization proposed by Ferrari and Robertson [24], the a-C film and a-C films with different G-N cap layers were in stage 2 ranging from amorphous carbon type to nanocrystalline type. The nanocrystallite size was proportional to the I_D/I_G. Fig. 2(a) shows run-in cycles and I_D/I_G of a-C film and a-C films with 5 nm-thick G-N cap layers prepared by different electron irradiation energies. The I_D/I_G increased with the increasing of

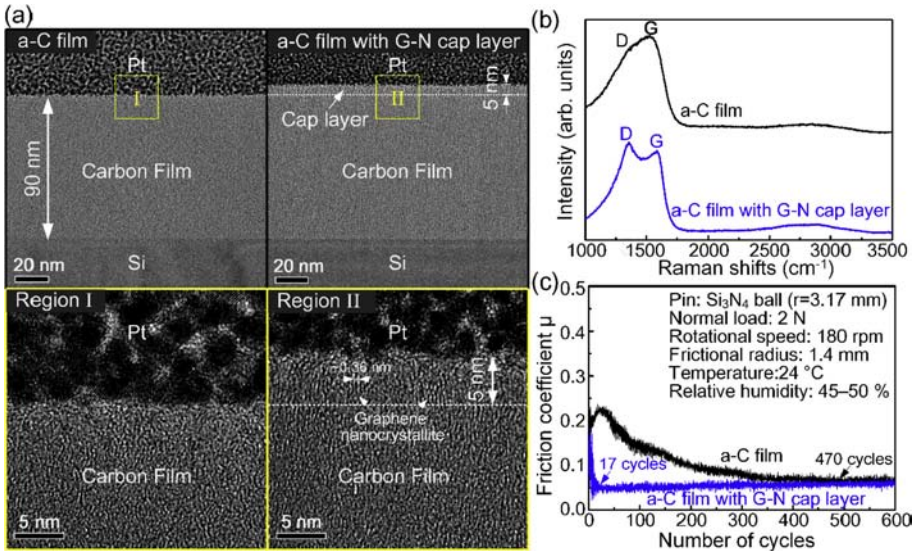

Fig. 1. (a) Cross-sectional view TEM images of a-C film and a-C film with G-N cap layer (electron irradiation energy, 40 eV; deposition time, 5 min). Region I and Region II were the enlargement of top surface nanostructure of the two carbon films. (b) Raman spectra and (c) typical friction curves of a-C film and a-C film with G-N cap layer. (A colour version of this figure can be viewed online.)

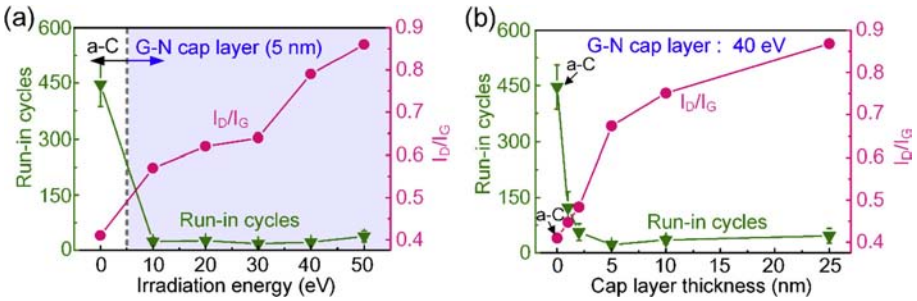

Fig. 2. (a) Run-in cycles and I_D/I_G of a-C film and a-C films with 5-nm-thick G-N cap layers prepared by different electron irradiation energies. (b) Run-in cycles and I_D/I_G of a-C film and a-C films with different thicknesses G-N cap layers prepared by 40 eV electron irradiation. (A colour version of this figure can be viewed online.)

irradiation energy, and the run-in cycles of the films sharply decreased with the existence of the G-N cap layer. Fig. 2(b) shows run-in cycles and I_D/I_G of a-C film and a-C films with different thicknesses G-N cap layers prepared by 40 eV electron irradiation. Run-in cycle distinctly decreased from 480 ± 160 cycles for the a-C film (G-N cap layer thickness is 0 nm) to 22 ± 5 cycles for the film with a 5 nm-thick G-N cap layer, then changed little with further increasing the thickness of G-N cap layer to 25 nm. I_D/I_G increased with G-N cap layer thickness, and the run-in cycles of the films decreased sharply with certain value of I_D/I_G. These results implied that the graphene nanocrystallite was the essential factor for the reduction of run-in period.

3.2. Nanostructure investigation of transfer film

In order to understand the different run-in behaviors of a-C film and a-C film with G-N cap layer (40 eV; 5 nm), the structures of worn scars on the Si_3N_4 ball surfaces after 30 cycles and 500 cycles were observed and analyzed with an optical microscope and Raman spectroscopy. The results are shown in Fig. 3. For the a-C film, the optical image of the ball surface after 30 sliding cycles could not find the existence of transfer film, and the corresponding Raman spectrum also had no carbon signal (G band). After 500 cycles sliding, friction coefficient reached stable low friction stage, weak D band and G band appeared separately in the Raman spectrum, indicating the formation of thin nanocrystallized transfer film. The corresponding optical image showed an indistinct transfer film on the ball surface. When the a-C film covered with a G-N cap layer, transfer film can be found on the ball surface only after 30 sliding cycles, which could be the reason for rapid reaching low friction stage. Further sliding for 500 cycles, the transfer film became more distinct and fully covered the contact area. In addition, the Raman spectra showed sharp D band, G band and 2D band, indicating the presence of graphene nanocrystallites in the transfer films [25–27]. And the degree of nanocrystallization of transfer film was higher than that of the cap layer. The above results demonstrated that the formation of transfer film coincided with low friction behavior, and the G-N cap layer helped to dramatically accelerate the formation of transfer film, thus the run-in period was greatly shortened.

The cross-sectional nanostructures of the transfer films of a-C film and a-C film with G-N cap layer after 500 cycles were observed with TEM. The results are shown in Fig. 4. It can be seen that both of the transfer films contained graphene nanocrystallites. The orientation of the graphene sheets in the transfer films was approximately parallel to the Si_3N_4 ball (sliding direction). And the nanocrystallization degree of the transfer film of a-C film with G-N cap layer was higher than that of the transfer film of a-C film, which is in accordance with the results of Raman spectra (Fig. 3). This observation gives a direct evidence for the low friction mechanism of the carbon films.

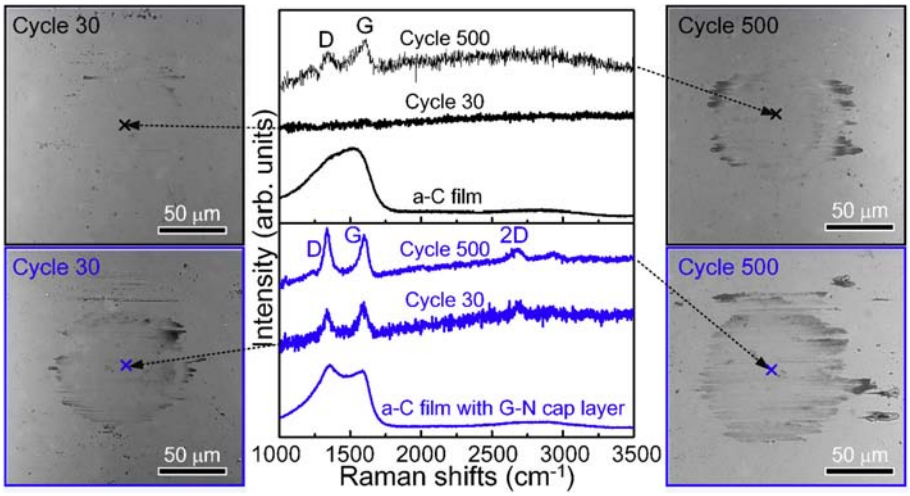

Fig. 3. Raman spectra and optical images of worn scars on the Si_3N_4 ball surfaces after 30 cycles and 500 cycles of the a-C film and a-C film with G-N cap layer (40 eV; 5 nm). (A colour version of this figure can be viewed online.)

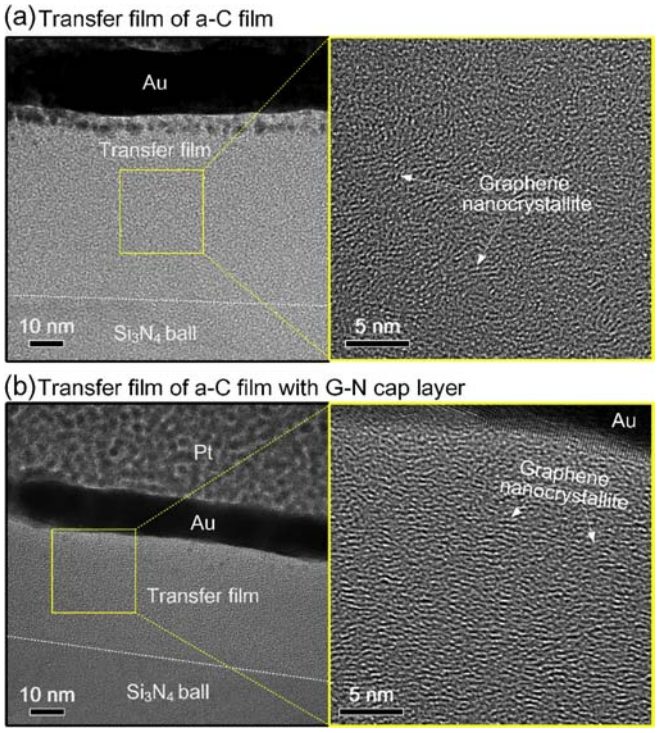

Fig. 4. Cross-sectional TEM images of transfer films after 500 cycles of (a) a-C film and (b) a-C film with G-N cap layer (40 eV; 5 nm). (A colour version of this figure can be viewed online.)

3.3. Nanoscratch and nanoindentation tests of carbon film

The raw materials for the formation of transfer films were primarily from the top surfaces of carbon films. The main difference between the two kinds of films was the graphene nanocrystallites embedded in the top surface for the a-C film with G-N cap layer. In order to uncover the causes for the different formation speed of the transfer films, nanoscratch tests were used to evaluate top-surface wear resistances of the carbon films in nanoscale. Fig. 5(a) shows nanoscratch depths of a-C film and a-C films with 5 nm-thick G-N cap layer prepared by different electron irradiation energies. The nanoscratch depths of the a-C films with G-N cap layer were all obviously higher than the a-C film. And the nanoscratch depth increased with the increasing of the cap layer thickness, as shown in Fig. 5(b). These indicate that the wear resistance of the G-N cap layer was lower than that of a-C film, which could be one cause of rapid formation of transfer film.

Nanoindentation tests were performed to evaluate the hardnesses of the carbon films. Fig. 6(a) shows load–displacement curves of a-C film and a-C films with different thicknesses of G-N cap layer. The maximum indentation load was 500 μN. The maximum penetration depths of the films were more than 30 nm, which was beyond the thickness of G-N cap layer and 20% of the film thickness. Therefore, the values of the hardnesses were considered as a mixture of G-N cap layer, a-C film and substrate [28,29]. Fig. 6(b) summarizes the hardnesses of a-C film and a-C films with different thicknesses of G-N cap layer. When the G-N cap layer thickness was lower than 10 nm, the hardness of a-C film with G-N cap layer was closed to that of a-C film, which means the fabrication of ultrathin G-N cap layer did not change the hardness of the underlying a-C film. As the G-N cap layer thickness increased to 25 nm, the contribution of the G-N cap layer to the value of hardness increased, and the hardness decreased to 13.2 ± 1.2 Gpa. This indicates that the hardness of the G-N cap layer was lower than that of a-C film, which is in accordance with the results of the nanoscratch tests.

3.4. Effect of annealing on nanostructure of carbon film

It should be noted that the formations of transfer films were accompanied with nanocrystallization, as shown in Fig. 2. The nanocrystallization is also a key factor for the decreasing of friction coefficient [10]. And it is often ascribed to friction-induced heat and/or friction-induced stress relaxation for the amorphous carbon film [7–12]. For the a-C film with G-N cap layer, it is meaningful to analyze the nanocrystallization mechanism for further clarifying the causes of short run-in period. Therefore, annealing experiments of 5 nm-thick a-C film and 5 nm-thick G-N film (40 eV) were performed to uncover the different nanocrystallization behaviors. Fig. 7 shows Raman spectra and I_D/I_G of 5 nm-thick a-C film and 5 nm-thick G-N film annealed at different temperatures. The D and G bands of 5 nm-thick a-C film became more distinct and the corresponding I_D/I_G increased obviously with the increasing of annealing temperature, as shown in Fig. 7(a, c), implying the

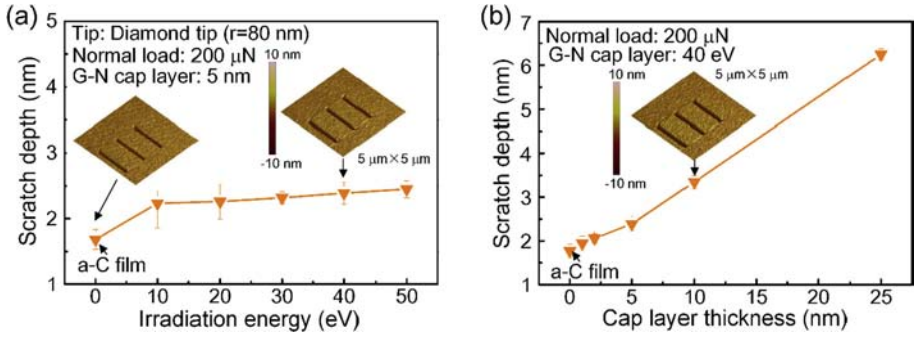

Fig. 5. (a) Nanoscratch depths of a-C film and a-C films with 5 nm-thick G-N cap layer prepared by different electron irradiation energies. (b) Nanoscratch depths of a-C film and a-C films with different thicknesses of G-N cap layer prepared by 40 eV electron irradiation. (A colour version of this figure can be viewed online.)

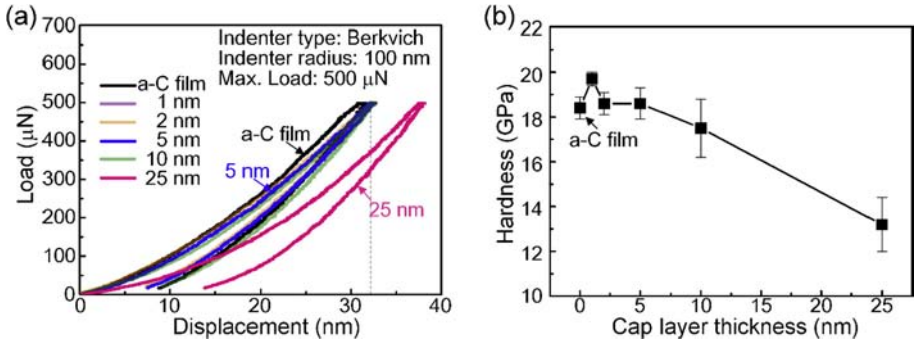

Fig. 6. (a) Load–displacement curves and (b) hardnesses of a-C film and a-C films with different thicknesses of G-N cap layer prepared by 40 eV electron irradiation. (A colour version of this figure can be viewed online.)

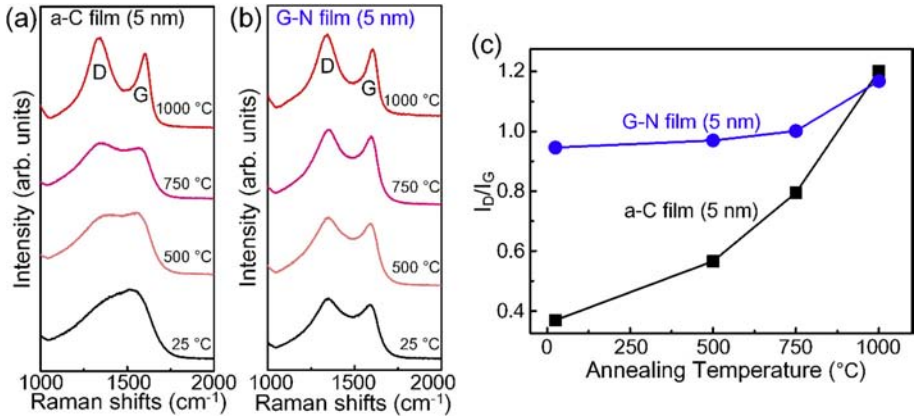

Fig. 7. Raman spectra of (a) 5 nm-thick a-C film and (b) 5 nm-thick G-N film (40 eV) annealed at different temperatures. (c) I_D/I_G of a-C film and G-N film annealed at different temperatures. (A colour version of this figure can be viewed online.)

transformation from amorphous to nanocrystallite. For the G-N film, the I_D/I_G stayed relatively constant up to 750 °C, then increased a little at 1000 °C, which reveals high thermal stability of graphene nanocrystallite. The friction-induced heat was about 200–600 °C [9,12]. So it can be deduced that the friction-induced heat played an important role on the nanocrystallization of a-C film, but had a negligible effect on the G-N cap layer. Therefore, for the a-C film with G-N cap layer, the nanocrystallization of transfer film was mainly attributed to friction-induced stress relaxation but not friction-induced heat. Furthermore, graphene nanocrystallites in the cap layer could directly serve as raw materials for the nanocrystallized transfer film, so the nanocrystallization of transfer film actually was friction-induced restructuring of graphene nanocrystallites.

3.5. Short run-in period mechanism

Based on the above nanoscratch, nanoindentation and annealing analysis, the short run-in period mechanism was interpreted that graphene nanocrystallite layer was easier to be worn out than amorphous carbon, severed as a sacrificial layer and helped to rapidly form the nanocrystallized transfer film by friction-induced restructuring of graphene nanocrystallite. Fig. 8 illustrates the short run-in period mechanism for amorphous carbon film with G-N cap

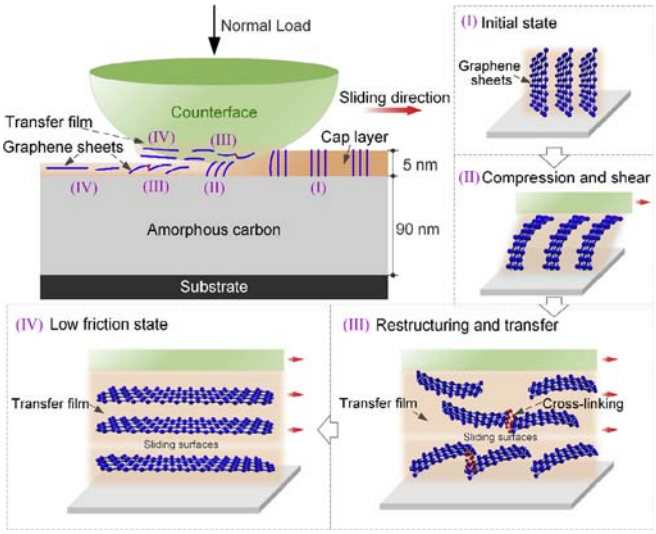

Fig. 8. Short run-in period mechanism: friction-induced rapid restructuring of graphene nanocrystallite cap layer. (I) Initial state of graphene sheets. (II) Compression and shear of graphene sheets with counterface. (III) Restructuring and transfer of graphene sheets under frictional sliding. (IV) Low friction state of graphene sheet sliding against graphene sheet. (A colour version of this figure can be viewed online.)

layer. Initially, nanosized graphene sheets are vertically aligned in the cap layer (stage I). The edge of graphene sheets are active [30] and prefer to form covalent bond with the counterface under compression and shear, leading to high friction at the beginning sliding (stage II). Since graphene sheet is the strongest in the 2D structures ever known and has extraordinary wear resistance [31,32]. During the sliding process, graphene sheets would be peeled off in forms of single or multi sheets rather than be worn in a mild homogeneous process, and tend to lay down and reorient towards the sliding direction. Graphene sheets accumulate at the sliding surfaces, giving rise to the formation of transfer film. In addition, local contact stress would induce cross-linking and connecting of graphene sheets [33], resulting in high degree of nanocrystallization of transfer film (stage III). Finally, the interaction between the sliding surfaces turns to be mainly low van der Waal force between graphene sheets (stage IV).

3.6. Effect of multilayer graphene micro-flake on run-in period

Multilayer graphene micro-flakes were also used to verify the short run-in period mechanism. Since it is parallel-aligned on the amorphous carbon film surface, further reduction of the run-in period may be expected. After frictional test, as shown in Fig. 9(a), the film with graphene flakes showed that friction coefficient rapidly decreased to ~0.06 in 10 cycles, but appeared fluctuation within the value of 0.10 for 200 cycles. Observing the worn scars on the Si_3N_4 ball surfaces with optical microscope, an obvious transfer film formed on the contact area only after 10 sliding cycles, and became thicker after 500 sliding cycles, as shown in Fig. 9(b, c). The Raman spectra of the transfer films showed that D bands intensity were dramatically increased compared with that of original Raman spectrum of the a-C film with graphene flakes, as shown in Fig. 9(d), which indicating the nanostructure of the transfer film were graphene nanocrystallite. In other words, the nanostructure of graphene was transformed to be graphene nanocrystallite after

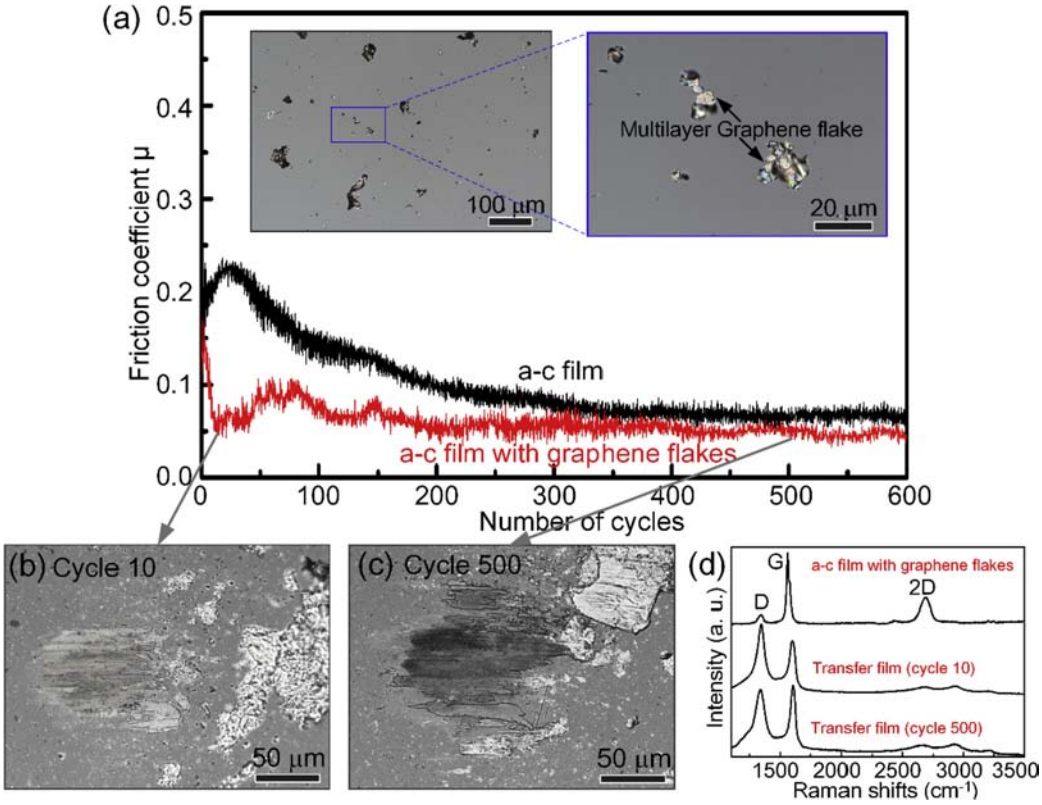

Fig. 9. (a) Typical friction curves of a-C film and a-C film with multilayer graphene flakes. Insets are the optical images of the surface of the a-C film with graphene flakes. (b, c) Optical images and (d) Raman spectra of worn scars on the Si_3N_4 ball surfaces after 10 cycles and 500 cycles of the a-C film with graphene flakes. (A colour version of this figure can be viewed online.)

sliding, which is the reason for the fluctuation of friction coefficient in the initial 200 cycles. Since graphene has high thermal stability [34], the structure transformation was ascribed to friction-induced stress. Therefore, a-C film covered with multilayer graphene micro-flakes also verified that friction-induced rapid restructuring of graphene sheets at sliding surfaces resulted in short run-in period. Furthermore, it interesting to expect that in order to certainly eliminate the run-in period of amorphous carbon film, a parallel-aligned and suitable-sized graphene nanocrystallite cap layer is needed.

4. Conclusions

In summary, we proposed a technique to shorten the frictional run-in period of amorphous carbon film by fabricating a thin graphene nanocrystallite cap layer. The dependences of run-in period on graphene nanocrystallite size and cap layer thickness implied that the graphene nanocrystallite was the key factor for the reduction of run-in period. The short run-in period mechanism was interpreted that graphene nanocrystallite layer was easier to be worn out than amorphous carbon, severed as a quick-wearing sacrificial layer and helped to rapidly form the nanocrystallized transfer film by friction-induced restructuring of graphene nanocrystallite. Besides, the frictional tests of amorphous carbon film covered with multilayer graphene micro-flakes also verified that friction-induced rapid restructuring of graphene sheets at sliding surfaces resulted in short run-in period.

Acknowledgements

The authors would like to thank the National Natural Science Foundation of China (Nos. 51705331 and 51575359), China Postdoctoral Science Foundation (No. 2016M600666), National Natural Science Foundation of Guangdong, China (No. 2016A030310041), and Shenzhen Fundamental Research and Discipline Layout Project (No. JCYJ20160427105015701). The authors thank Dr. Meijie Yin and Electron Microscopy Center of Shenzhen University for the help in TEM observations of transfer films.

References

[1] A. Erdemir, C. Donnet, Solid lubricant coatings: recent development and future trends, Tribol. Lett. 17 (3) (2004) 389–397.
[2] K. Bewilogua, D. Hofmann, History of diamond-like carbon films-From first experiments to worldwide applications, Surf. Coating. Technol. 242 (2014) 214–225.
[3] S.V. Hainsworth, N.J. Uhure, Diamond like carbon coatings for tribology: production techniques, characterisation methods and applications, Int. Mater. Rev. 52 (3) (2007) 153–174.
[4] D. Berman, S.A. Deshmukh, S.K.R.S. Sankaranarayanan, A. Erdemir, A.V. Sumant, Macroscale superlubricity enabled by graphene nanoscroll formation, Science 348 (2015) 1118–1122.
[5] X. Fan, D.F. Diao, Contact mechanisms of transfer layered surface during sliding wear of amorphous carbon film, ASME J. Tribol. 133 (2011), 042301.
[6] Z.B. Gong, J. Shi, B. Zhang, J.Y. Zhang, Graphene nano scrolls responding to superlow friction of amorphous carbon, Carbon 116 (2017) 310–317.
[7] Y. Liu, E.I. Meletis, Evidence of graphitization of diamond-like carbon films during sliding wear, J. Mater. Sci. 32 (1997) 3491–3495.
[8] S. Miyai, T. Kobayashi, T. Terai, Mechanical, thermal, and tribological properties of amorphous carbon films, Jpn. J. Appl. Phys. 48 (2009), 05EC05.
[9] G. Sutter, N. Ranc, Flash temperature measurement during dry friction process at high sliding speed, Wear 268 (2010) 1237–1242.
[10] T.B. Ma, Y.Z. Hu, H. Wang, Molecular dynamics simulation of shear induced graphitization of amorphous carbon films, Carbon 47 (2009) 1953–1957.
[11] A.P. Merkle, A. Erdemir, O.L. Eryilmaz, J.A. Johnson, L.D. Marks, In situ TEM studies of tribo-induced bonding modifications in near-frictionless carbon films, Carbon 48 (2010) 587–591.
[12] D.S. Wang, S.Y. Chang, Y.C. Huang, J.B. Wu, H.J. Lai, M.S. Leu, Nanoscopic observations of stress-induced formation of graphitic nanocrystallites at amorphous carbon surfaces, Carbon 74 (2013) 302–311.
[13] T.W. Scharf, I.L. Singer, Role of the transfer film on the friction and wear of metal carbide reinforced amorphous carbon coatings during run-in, Tribol. Lett. 36 (2009) 43–53.
[14] C. Donnet, A. Erdemir, Tribology of diamond-like carbon films: fundamentals and applications, in: H. Ronkainen, K. Holmberg (Eds.), Environmental and Thermal Effects on the Tribological Performance of DLC Coatings, Springer, New York, 2008, pp. 155–200.
[15] Y. Liu, E.I. Meletis, An investigation of the relationship between graphitization and frictional behavior of DLC coatings, Surf. Coating. Technol. 86–87 (1996) 564–568.
[16] D.W. Kim, K.W. Kim, Effects of sliding velocity and normal load on friction and wear characteristics of multi-layered diamond-like carbon (DLC) coating prepared by reactive sputtering, Wear 297 (2013) 722–730.
[17] J. Fontaine, T.L. Mogne, J.L. Loubet, M. Belin, Achieving superlow friction with hydrogenated amorphous carbon: some key requirements, Thin Solid Films 482 (2005) 99–108.
[18] M.J. Marino, E. Hsiao, Y.S. Chen, O.L. Eryilmaz, A. Erdemir, S.H. Kim, Understanding run-in behavior of diamondlike carbon friction and preventing diamond-like carbon wear in humid air, Langmuir 27 (2011) 12702–12708.
[19] A.A. Al-Azizi, O. Eryilmaz, A. Erdemir, S.H. Kim, Surface structure of hydrogenated diamond-like carbon: origin of run-in behavior prior to superlubricious interfacial shear, Langmuir 31 (2015) 1711–1721.
[20] K.P. Shaha, Y.T. Pei, D. Martinez-Martinez, JThM De Hosson, Influence of surface roughness on the transfer film formation and frictional behavior of TiC/a-C nanocomposite coatings, Tribol. Lett. 41 (2011) 97–101.
[21] R.R. Chromik, A.L. Winfrey, J. Luning, R.J. Nemanich, K.J. Wahl, Run-in behavior of nanocrystalline diamond coatings studied by in situ tribometry, Wear 265 (3–4) (2008) 477–489.
[22] X. Fan, D.F. Diao, W. Kai, W. Chao, Multi-functional ECR plasma sputtering system for preparing amorphous carbon and Al–O–Si films, Surf. Coating. Technol. 206 (2011) 1963–1970.
[23] C. Wang, D.F. Diao, X. Fan, C. Chen, Graphene sheets embedded carbon film prepared by electron irradiation in electron cyclotron resonance plasma, Appl. Phys. Lett. 100 (2012), 231909.
[24] A.C. Ferrari, J. Robertson, Interpretation of Raman spectra of disordered and amorphous carbon, Phys. Rev. B 61 (2000) 14095–14106.
[25] D. Graf, F. Molitor, K. Ensslin, C. Stampfer, A. Jungen, C. Hierold, et al., Spatially resolved Raman spectroscopy of single- and few-layer graphene, Nano Lett. 7 (2007) 238–242.
[26] L.M. Malard, M.A. Pimenta, G. Dresselhaus, M.S. Dresselhaus, Raman spectroscopy in graphene, Phys. Rep. 473 (5–6) (2009) 51–87.
[27] W. Chao, X. Zhang, D.F. Diao, Nanosized graphene crystallite induced strong magnetism in pure carbon films, Nanoscale 7 (2015) 4475–4481.
[28] B. Jönsson, S. Hogmark, Hardness measurements of thin films, Thin Solid Films 114 (1984) 257–269.
[29] B. Bhushan, Chemical, mechanical and tribological characterization of ultra-thin and hard amorphous carbon coatings as thin as 3.5 nm: recent developments, Diam. Relat. Mater. 8 (1999) 1985–2015.
[30] J.K. Xiao, L. Zhang, K.C. Zhou, J.G. Li, X.L. Xie, Z.Y. Li, Anisotropic friction behavior of highly oriented pyrolytic graphite, Carbon 65 (2013) 53–62.
[31] Y.H. Huang, Q.Z. Yao, Y.Z. Qi, Y. Cheng, H.T. Wang, Q.Y. Li, et al., Wear evolution of monolayer graphene at the macroscale, Carbon 115 (2017) 600–607.
[32] D. Berman, S.A. Deshmukh, S.K.R.S. Sankaranarayanan, A. Erdemir, A.V. Sumant, Extraordinary macroscale wear resistance of one atom thick graphene layer, Adv. Funct. Mater. 24 (2014) 6640–6646.
[33] Q. Zhang, D.F. Diao, L. Yang, Dangling bond induced cross-linking model in nanoscratched graphene layers, Surf. Coating. Technol. 237 (2013) 230–233.
[34] A.E. Galashev, O.R. Rakhmanova, Mechanical and thermal stability of graphene and graphene-based materials, Phys. Usp. 57 (2014) 970–989.